

# Design of the unit telescopes of the MROI

Olivier Pirnay, Pierre Gloesener, Eric Gabriel, Vincent Moreau, François Graillet, Christophe Delrez

Advanced Mechanical and Optical Systems (AMOS s.a.),  
Parc Scientifique du Sart-Tilman, B-4031 ANGLEUR (Liège), BELGIUM

## ABSTRACT

AMOS is in charge of the development of the unit telescopes of the MRO interferometer. Beyond the image quality and the tracking performance, the interferometry necessitates maintaining the optical pathlength between two telescopes sufficiently stable during observation. This paper depicts the detailed design of the telescopes and how it suits to the high end requirements of the system. The distinctive features of the elevation over elevation configuration are also discussed.

**Keywords:** telescope, interferometry, optical array, optical path length stability, afocal, elevation over elevation

## 1. INTRODUCTION

The Magdalena Ridge Observatory Interferometer (MROI) is a high-sensitivity imaging optical/IR interferometer in construction on the Magdalena Ridge. It is situated at the altitude of 3230 m, 45 km West of Socorro, NM.

Up to 10 unit telescopes will be operated simultaneously to produce model-independent images. These telescopes can be relocated on 28 different piers spread on a "Y" shape array. With baselines from 7.5 m to 340 m, the instrument will generate sub-milliarcsecond angular resolution sharp images in the range of 0.6 to 2.4  $\mu\text{m}$  wavelength.

The instrument optical throughput is optimized in order to image faint objects: one key piece is the 1.4 m unit telescope in which the stellar light is collected only with three mirrors thanks to the afocal elevation over elevation configuration.

The major science goals are the study of the earliest phases of star and planet formation, the complex astrophysical processes in single and multiple star systems, and the environments of black holes in the hearts of other galaxies.

The MRO Interferometer project is co-funded by the Naval Research Laboratory (NRL), the New Mexico Institute of Mining and Technology (NMT) in Socorro, NM and the University of Cambridge's Cavendish Laboratory in England.

AMOS signed in July 2007 the contract with NMT for the development of the unit telescopes of the MRO interferometer. The design phase will be completed in October 2008.



Fig. 1. Artistic view of the MROI Interferometer: the buildings construction was completed in 2007. The array is under construction. (Courtesy of MRO)

The contract between AMOS and NMT covers the design and manufacturing of the unit telescopes. This includes the structures, the drives, electronics and mechanisms, the telescope control system and the mirrors supporting devices. The mirror manufacturing is out of the scope of AMOS contract. AMOS is also in charge of the design of the interface with the pier and the tools necessary for the installation and the alignment of the 28 telescope stations on the array.

## 2. REQUIREMENTS SPECIFICATION

The telescope is a Mersenne beam compressor supported by an elevation-over-elevation mount. The system consists in a 1425 mm diameter  $f/2.25$  concave parabolic primary combined with a 115 mm diameter convex parabolic secondary. The M1-M2 spacing is 2936.25 mm. The 95 mm diameter collimated beam is sent out of the telescope through the outer elevation axis thanks to a flat mirror (M3) rotating around the inner elevation axis. The tracking speed of the M3 is half of the speed of the inner elevation axis. The angular range (field of regard) is respectively  $-50/+40$  degrees and  $\pm 60$  degrees from zenith for the inner elevation axis and the outer elevation axis.

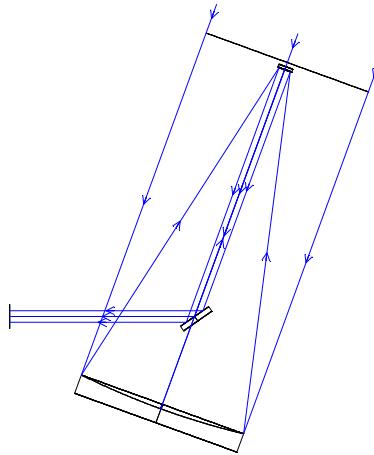


Fig. 2. Optical configuration of the MROI unit telescope.

The ambitious objectives of the MRO Interferometer led the system architects to specify stringent requirements for the unit telescope. The performance summarized here below will be maintained in severe environmental conditions.

- Overall image quality: 63 nm RMS
- Optical obscuration less than 5%
- Pupil stability: 0.5 mm over the entire field of regard
- Pointing error less than 20 arcsec over the full night
- Open loop tracking better than 1 arcsec
- Closed loop tracking: 0.02 arcsec and 0.03 arcsec RMS respectively for the mount and the wind shake residual error. A 200 Hz bandwidth fast steering actuator is implemented at the level of the secondary mirror for tip-tilt correction.
- Optical Path Length (OPL) Stability: 23 nm RMS for a 12 ms exposure time frame

## 3. DESIGN OVERVIEW

The afocal telescope is implemented in an elevation over elevation mount. The two axes are connected to each other by means of a gimbal structure. The fork is the fixed part of the telescope. It supports the outer elevation axis of the gimbal and provides a stiff and stable interface with the pier. The fork also provides the interface for the Nasmyth table where the closed loop sensors are installed by the final user. The gimbal is a closed frame box structure. It locates the two main axes concurring and perpendicular to each other. It supports the telescope tube through the inner elevation axis. The tube supports and maintains stable the optics in the entire operational range. The tube supports the M2 and M3 units. It also

provides a mechanical interface for the primary unit. The M1 unit consists in the primary mirror and its supporting cell. The cell maintains the mirror in shape and position. The M1 cell is fixed to the tube.

The control system of the telescope allows to move the axis in the way to point and to track the targets. The main electronics are located in the enclosure in order to minimize the thermal load in the vicinity of the light beam.

Total weight: 15 500 kg – Overall dimensions (L x W x H): 6160 x 2920 x 4350 mm

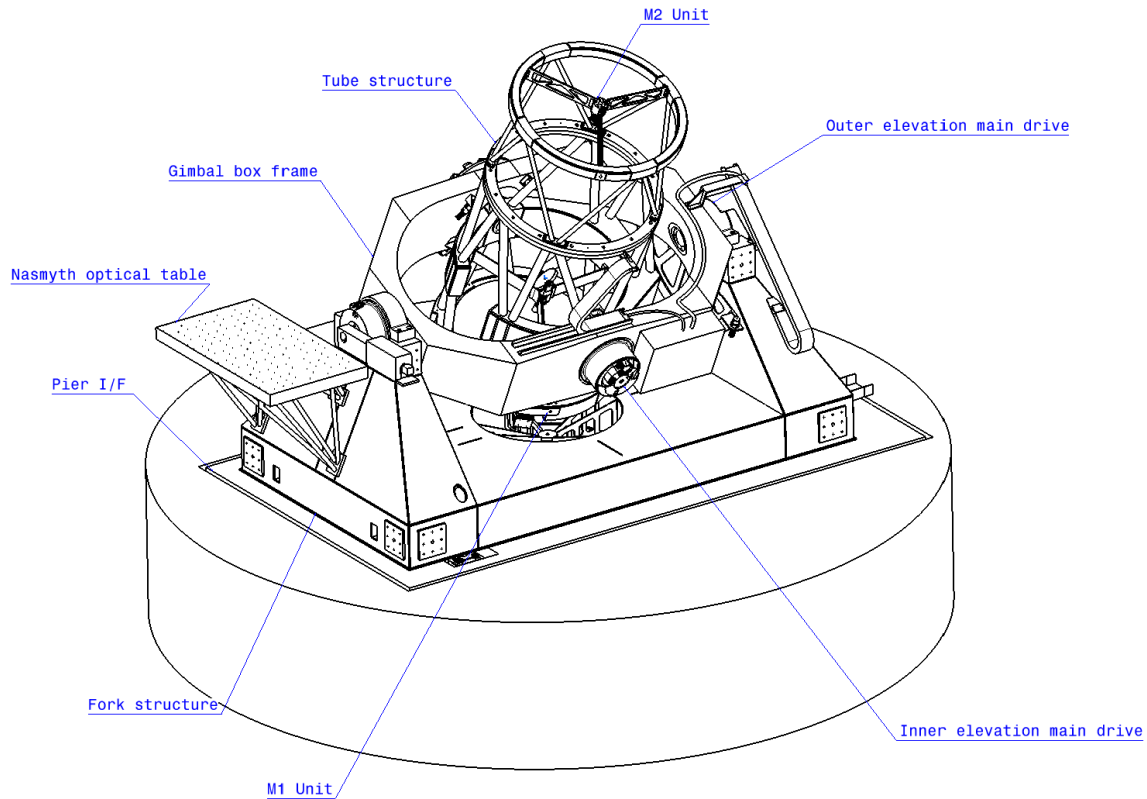


Fig. 3. MROI unit telescope, overall view.

The elevation-over-elevation configuration necessitates having an opening in the tube to avoid obscuration of the output beam. As a consequence, the tube geometry becomes unsymmetrical and the truss structure is not acting as a perfect Serrurier. Another feature of this configuration is the variable inclination of the tube in both directions; an important optimization process is necessary to bring the static deflection of the structure to an acceptable level.

### 3.1 M1 unit

The M1 unit is the primary mirror and its supporting cell. The cell maintains the mirror in shape and position. The primary mirror manufacturing is out of the scope of AMOS work. AMOS designs the shape and position of the pads that will be glued on the mirror.

Total weight of the supporting cell: 715 kg (supporting a mirror of 650 kg)

Size: Ø 1800 / height: 500 mm

The supporting of the mirror is designed as an externally quasi-isostatic system, i.e. six and only six independent degrees of freedom are constrained: one central pivot point, one axial support resulting from three vertical fixation points and one tangential fixation point. The quasi-isostatic quality of the support is the key feature of a mirror support but the complete

assembly shall remain sufficiently stiff and stable in position. The support is fully passive. The structure is optimized for the stiffness. The integration accessories are built-in to ease the mirror installation/removal for coating.

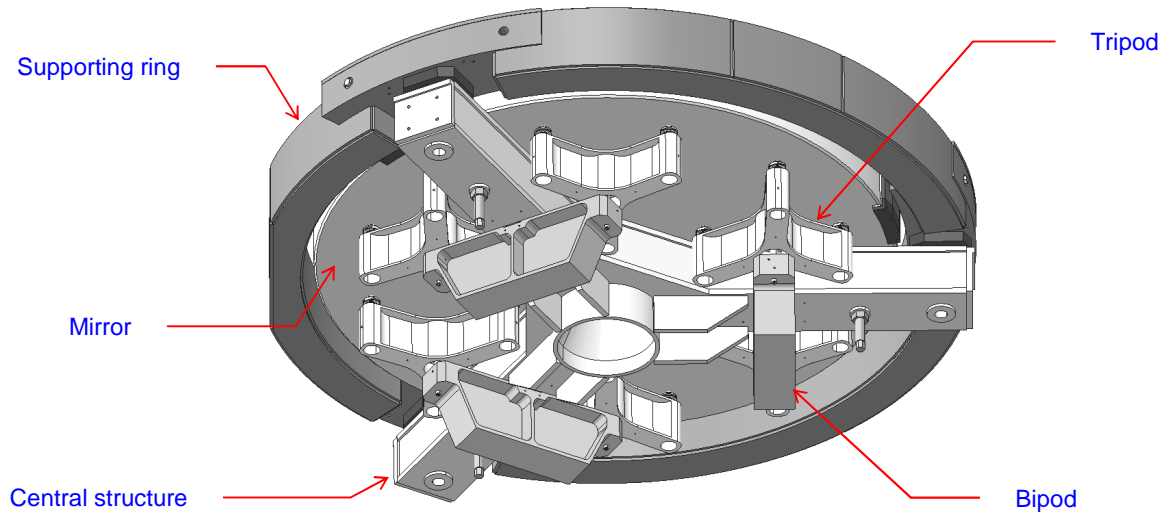


Fig. 4. M1 unit, general view from the bottom

The axial support is an 18-point quasi-isostatic support distributed on two stages above each of the three fixed points: one bipod and two tripods. Six needles make the connection between the tripods and the mirror.

The central point acts as a pivot: it locates the mirror laterally and –as a radial support- takes back the fraction of the gravity load acting in the direction normal to the optical axis of the mirror. Basically, the central point is a membrane connected externally to the mirror central hole and internally to the structure. The choice of a central supporting rather than astatic radial levers is driven by the fact that the gravity load acts in any direction.

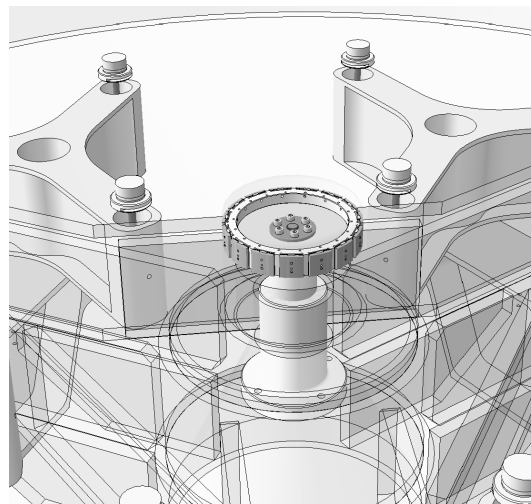


Fig. 5. M1 Unit, radial support (seen through the mirror)

The dimensioning criteria for the support are the optical surface deformation in operation and the stress in materials under extreme environmental conditions. The proper dimensioning of the supporting is performed by the finite element analysis (FEA) and post-processed by means of software tools developed by AMOS. The residual mirror surface deformation due to the supporting is as follows:

*Axial supporting* (gravity in the direction of the optical axis): **3.3 nm RMS surface**, (tilt-focus terms removed)

*Lateral supporting* (gravity perpendicular to the optical axis): **3.8 nm RMS surface**, (tilt-focus-coma terms removed)

The focus and coma aberrations are compensated by applying the equivalent correction at the level of M2 mechanism.

### 3.2 Tube

The tube supports and maintains the optics stable. It is connected to the gimbal through the inner elevation bearings. The tube supports the M2 unit, the M3 unit and the finder telescope. It also provides a mechanical interface for the primary unit. The manufacturing tolerances and alignment capabilities provided on the tube allow to set-up the proper mirror combination and locate the optical axis of the telescope with respect to the mount axes.

Total weight (incl. spiders) : approx. 2400 kg

Size: Ø 1900 / height: 3300 mm

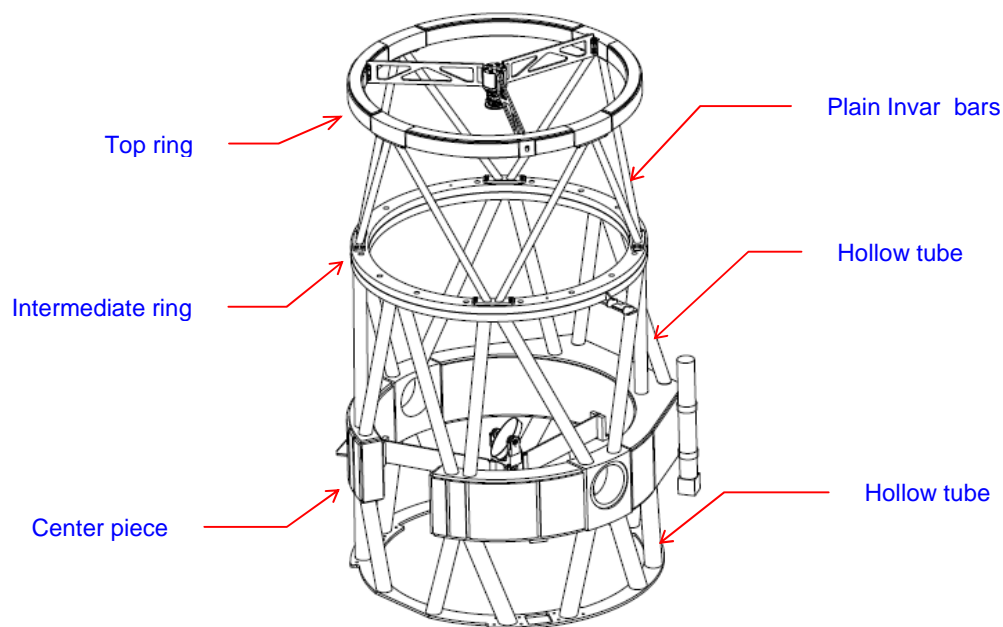


Fig. 6. Tube, general view

The tube is composed of a center piece, a lower ring, an intermediate ring and a top ring. The rings are connected by means of hollow and plain tube trusses. The distance between the lower ring and the intermediate ring has been minimized in order to keep the structure as stiff as possible. The center piece is a horseshoe-shaped box frame. The section of the box frame is variable in order to increase the stiffness. The truss structure is also not symmetrical to accommodate the opening for the output beam.

The tube structure is made of low carbon steel, except for the top tubes, connecting intermediate ring and top ring. In order to reduce the global expansion of the telescope during an observation, the top tubes are made of Invar<sup>®</sup> to decrease

the influence of an air temperature change. During a 5 minute period of acquisition, the maximum defocus due to temperature change is lower than 1.5  $\mu\text{m}$ .

### 3.3 M2 Unit

The M2 unit is composed of the M2 mirror and a supporting cell. It is mounted on a dual stage positioning mechanism: a low-bandwidth mechanism -a hexapod- compensates for the aberration arising during operation and a fast tip-tilt mechanism allows correction up to 50 Hz.

The fast steering of the secondary necessitates limiting the inertia of the mirror. The light-weighting and supporting configuration was determined by FEA. The mirror manufacturing is out of the scope of the AMOS contract with NMT. The residual mirror surface deformation due to the supporting is as follows:

*Axial supporting* (gravity in the direction of the optical axis): **0.9 nm RMS surface**

*Lateral supporting* (gravity perpendicular to the optical axis): **2 nm RMS surface**

*Thermal load case* ( $\Delta T = -35^\circ\text{C}$ ): **0.93 nm RMS surface**, (focus term removed)

### 3.4 M2 mechanism

The first stage of the M2 mechanism is a hexapod. One fraction of the hexapod range is used to set-up the initial alignment of M2 when the telescope is installed on the station for the first time and every time the calibration sequence is run. During a typical observation night, the hexapod M2 position will be adjusted to maintain the image quality during acquisition. The command will be determined upon the tube temperature measurement and the compensation law for the aberrations due to the tube deflection under gravity load.

The compactness and stiffness requirements lead to design the hexapod system as a fixed length legs system. Six fixed length struts are connected to six parallel linear actuators at the backside. The other ends of the struts are connected to the moving platform. The configuration of the system provides high resolution motions in six independent directions.

The linear actuator is a mechanically preloaded spindle connected to a brushless motor. Limit switches and the magnetic encoder are integrated in the actuator. The non-reversibility of the mechanism will be guaranteed either by the spindle design either by the implementation of the fail-safe brake (powered on during the activation of the mechanisms). The actuators and the joints are designed and manufactured to avoid any backlash.

Table 1. M2 hexapod requirements specification

	Focus	Centering	Tip/Tilt
Travel range	$> \pm 1.5 \text{ mm}$	$> \pm 0.75 \text{ mm}$	$> \pm 5 \text{ arcmin}$
Accuracy	$< 1 \mu\text{m}$ diff. over $250 \mu\text{m}$ $< 0.5 \mu\text{m}$ diff. over $50 \mu\text{m}$	$< 20 \mu\text{m}$ abs.	$< 10 \text{ arcsec}$ diff. over $70 \text{ arcsec}$
Min. Incremental Motion	$< 0.2 \mu\text{m}$	$< 12 \mu\text{m}$ (goal $2 \mu\text{m}$ )	$< 10 \text{ arcsec}$ (goal $2 \text{ arcsec}$ )
Time response (time/step)	$< 2\mu\text{m} / 1 \text{ s}$	$< 100 \mu\text{m} / 10 \text{ s}$	$< 10 \text{ arcsec} / 10 \text{ s}$
Cross-coupling	$< 1 \text{ arcsec}$ tilt / $5\mu\text{m}$ step	-	-

### 3.5 M2 Fast tip-tilt

The second stage of the M2 mechanism is a closed loop piezo tip-tilt system (stroke  $> 100 \text{ arcsec}$  / resolution  $< 0.1 \text{ arcsec}$ ). The closed loop bandwidth is 50 Hz. The motion is measured by integrated capacitive sensors which allow the control electronics to compensate for hysteresis of the piezo. The hysteresis is than expected to be better than 1%. The tip-tilt pivot point will be as close as possible to the platform center of gravity in order to limit the inertia along the axis of rotation. The dynamics of the system -up to 200 Hz- will introduce some perturbations into the structure during operation. The impact on the OPL stability is evaluated in order to determine the need of a momentum compensation platform.

### 3.6 M3 Unit and mechanism

The M3 cell is designed to maintain the surface of the mirror in shape and to keep it stable in position with respect to its rotation. The mirror and its support are fixed onto the rotating element of the mechanism. The residual mirror surface deformation due to the supporting is as follows:

*Axial supporting* (gravity in the direction of the optical axis): **1.9 nm RMS surface**

*Lateral supporting* (gravity along the parabola long axis): **0.9 nm RMS surface**

*Thermal load case* ( $\Delta T = -35^{\circ}\text{C}$ ): **0.2 nm RMS surface**

The function of the M3 mechanism is to rotate the M3 optical surface around the M3 rotational axis of the telescope at half of the tracking speed. The mirror is initially aligned so that the M3 rotational axis lies in the plane of the mirror surface. The M3 axis of rotation is then aligned in a way that it is coincident with the inner elevation axis.

The rotational degree of freedom is accomplished by the implementation of a set of thin-section preloaded high-precision bearings, on each side of the mirror. These bearings are mounted on shafts between the cradle and the bearing carrier.

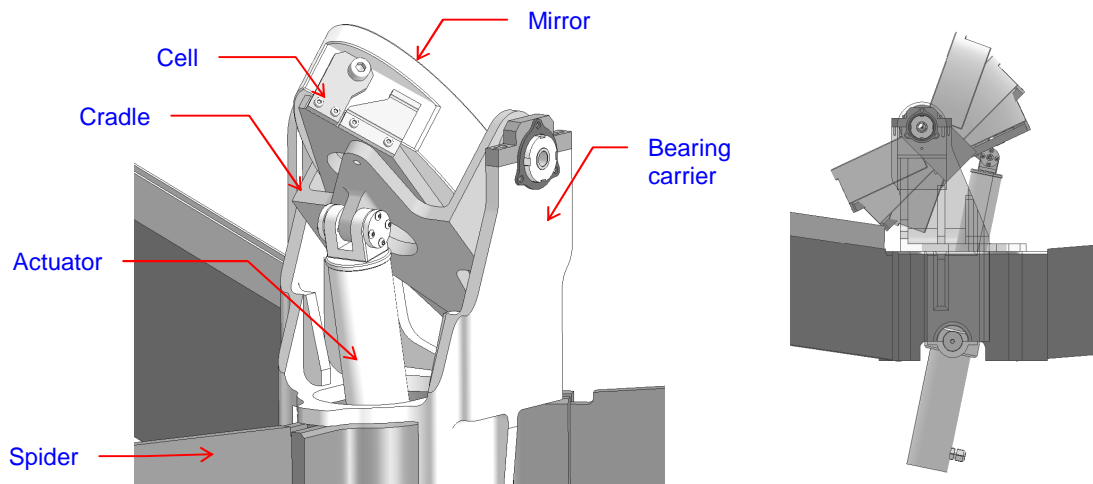


Fig. 7. M3 mechanism and mirror. General view from the rear (left) and side view (right) with the mirror represented in the outmost and median position

The linear actuator underneath the M3 cradle moves the mirror in the range  $+20^{\circ}/-25^{\circ}$  wrt the nominal position (when the telescope is pointing towards zenith). The attachment of the actuator to the M3 cradle and the bearing carrier is optimized from the point of view of angular resolution of the mirror and linear resolution of the actuator, as well as forces and force distribution over the operational angular range.

The connection between the actuator and the mirror support is accomplished by a needle roller bearing to avoid lateral loads on the actuator. The connection between the actuator and the bearing carrier is accomplished by two sets of preloaded angular contact ball bearings, in order to take up radial, axial and momentum load.

Table 2. M3 actuator requirements specification

	M3 stage	Linear Actuator
Travel range	$+22.5 \text{ deg} / -27.5 \text{ deg}$	$> 78 \text{ mm}$
Accuracy	$< 1 \text{ arcsec RMS over } 2.5 \text{ arcmin}$ $< 10 \text{ arcsec RMS over the full range}$	$< 0.30 \text{ }\mu\text{m RMS over } 50 \text{ }\mu\text{m}$ $< 3 \text{ }\mu\text{m RMS over the full range}$
Tracking speed	$\pm 7.5 \text{ arcsec/sec, direction inversion}$	$\pm 2.5 \text{ }\mu\text{m /s, direction inversion}$
Slewing speed	$1 \text{ deg/sec}$	$1.8 \text{ mm/s}$

The linear actuator is a ball screw coupled to a reduction gear and a DC motor. One encoder is installed on the shaft of the motor and another one of higher resolution and accuracy is installed directly on the M3 axis. The first one provides the feedback for the speed control loop and the second for the position control loop.

### 3.7 Gimbal Structure

The gimbal locates the two main axes concurring and perpendicular to each other. It is supported by the fork through the outer elevation axis bearings. It supports the tube through the inner elevation axis.

Weight: approx 3500 kg

Size (LxWxH): 3800 x 2300 x 800 mm

The gimbal is a welded box frame structure. Thanks to the unique shape of the ring, it was possible to support the gimbal on both ends by means of medium size ball bearings without limiting the field of regard. The closed ring shape makes the telescope stiff in both directions and easy to manufacture.

The complex shape of this structure originates from the necessity to be balanced within two directions. For this purpose, the structure exhibits a rotational symmetry along the inner elevation axis.

The gimbal is made of low carbon steel. Different thicknesses of steel are used with the criteria of maximizing the first frequencies. The first eigen mode of the gimbal is a mode of torsion around the outer axis that occurs at 18 Hz (locked rotor simulation).

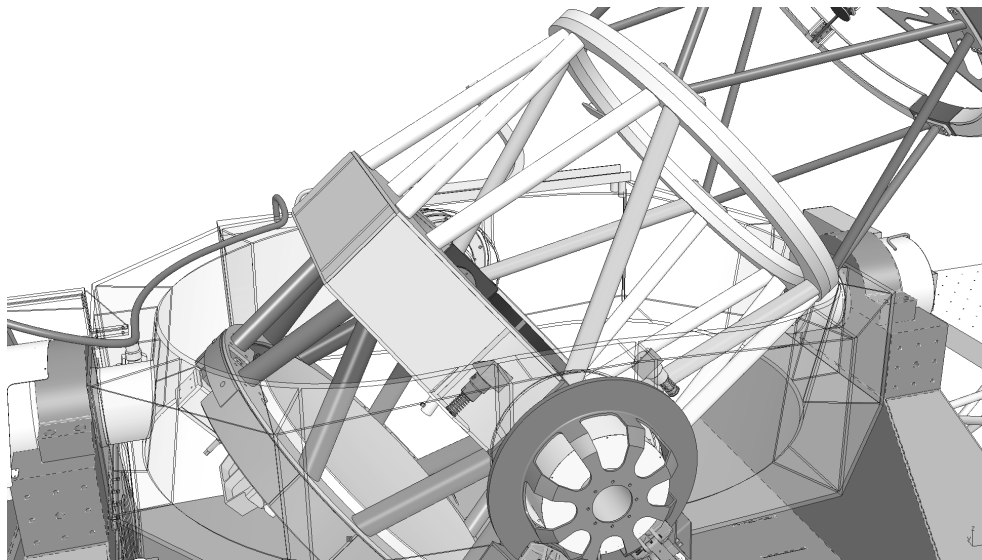


Fig. 8. Gimbal structure (represented semi-transparent). The inner axis to the utmost position.

### 3.8 Drives, Bearings and Safety Devices

The tube is supported by two pairs of medium size preloaded angular contact ball bearings. This configuration exhibits a good radial and transverse stiffness. It is designed in such a way that the load is divided optimally over the different bearings.

The main motors are rotary direct drive type mounted on the altitude shaft. The direct drive is the best choice for a system dedicated to interferometry: no irregularities in the motion due to the gear geometrical imperfections, no backlash, no stick-slip effect at tracking speed and no friction originating from the drive. It contributes to the good dynamic behavior of the electro-mechanical system with a low level of vibration affecting the OPL stability. One motor is mounted on each side of the tube to evenly apply the torque to the tube.



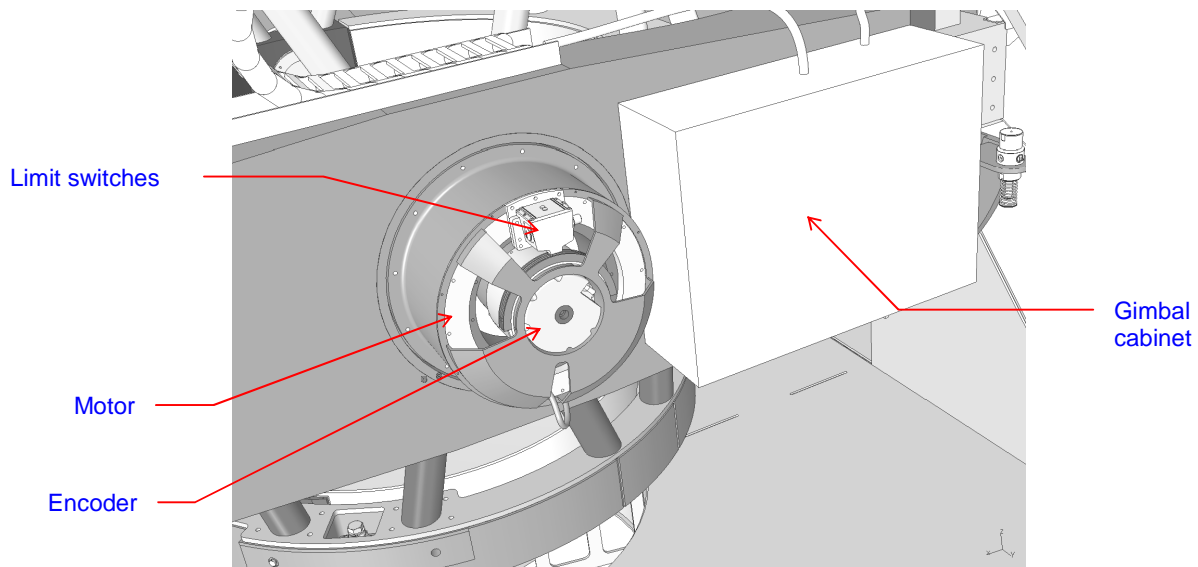


Fig. 9. Inner elevation axis arrangement

One high accuracy encoder is placed on the axis. This encoder will be rigidly coupled to the altitude axis behind the motor. The position sensors and power off limit switches are mounted on the axis. Fail-safe brakes and hydraulic dampers insure to safely stop the telescope in any circumstance.

The same configuration is used for the outer elevation axis with the same components except for the size of the bearing.

### 3.9 Fork Structure

The fork supports the gimbal through the outer elevation axis and provides a stiff and stable interface with the pier. The fork also provides the interface for the enclosure and fixation points for the Nasmyth table.

Weight: approx: 7400 kg

Size (LxWxH): 5000 x 2800 x 2000 mm

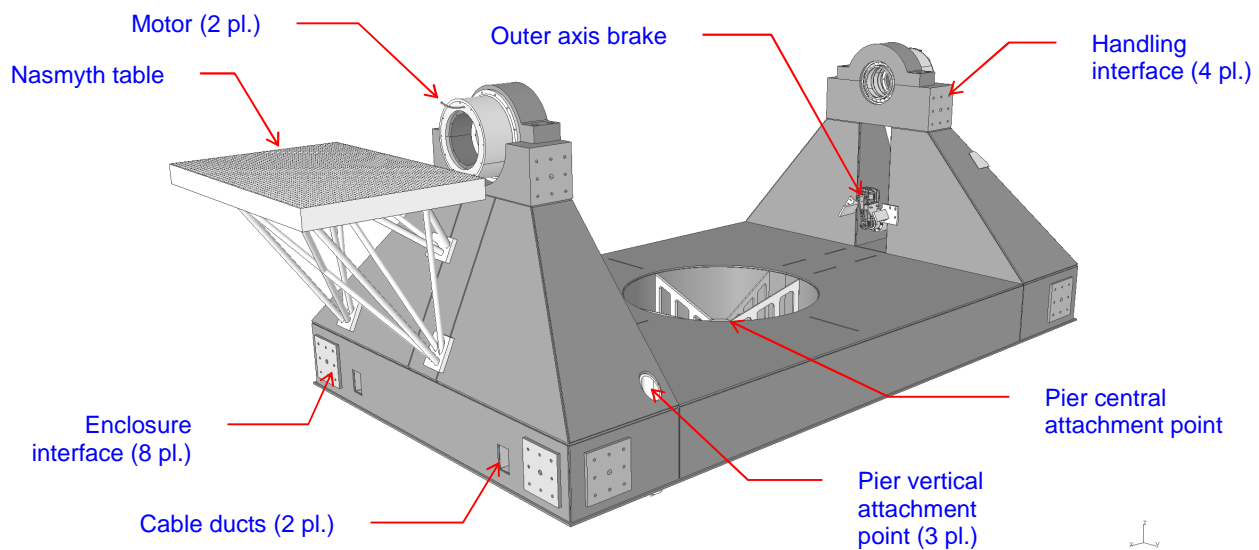


Fig. 10. Fork structure

The fork is a box frame welded structure. The thickness of the steel plates is differentiated (not homogeneous) in order to have the first natural frequencies higher than 17 Hz (locked rotor mode).

The accurate positioning of the outer elevation axis wrt the pier interface is provided by a machining of the two bearing bores after the machining of the pier interface on a large milling machine. The interface for the enclosure is machined at the same time. No additional alignment is required during the assembly with the gimbal.

Two cable ducts are integrated in the lower part of the fork for to ease the routing of the cables.

### 3.10 Pier Interface

The interface with the pier is designed as a kinematic supporting in order to avoid inducing stress and deformation to the telescope structure in case of misalignment or instability of the pier interface. The interface is composed of three vertical mating points, one lateral centering (2 directions) under the pivot point of the telescope and one lateral location in line with the output beam.

A large opening is provided at the centre of the fork to access to the central fixation point of the telescope situated vertically under the pivot point. The lateral fixation point is installed on the side opposite to the Nasmyth table, on an external bracket. These two points necessitate not more than a visual access during the installation on the pier. The vertical fixation points require an access from the top for fastening the screws.

The central and the lateral fixation points are accurately positioned wrt the fork axis thanks to a precise machining of the fork. The vertical fixation points can accommodate a lateral misalignment of the corresponding point of the pier up to  $\pm 20$  mm.

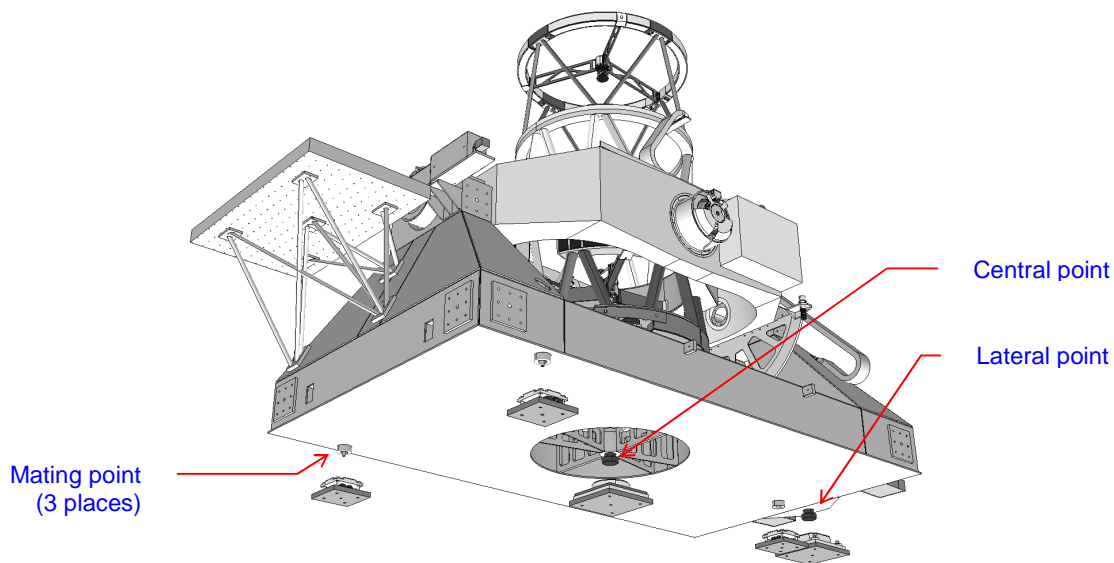


Fig. 11. Pier Interface, view from Bottom

### 3.11 Telescope Control System & Electronics

The computer dedicated to the telescope control, the programmable logic controller, the main axis controller and the outer axis amplifier are housed in the main electrical cabinet installed in the telescope enclosure. The inner axis drive, the hexapod and fast tip-tilt controllers are installed in a smaller cabinet attached to the gimbal. The temperature inside and on the outer skin of the gimbal cabinet is controlled thanks to a built-in liquid-air heat exchanger.

The unit telescope control system (UTCS) is developed under LabView<sup>®</sup> environment by Observatory Sciences Ltd<sup>[4]</sup>. The kernel of the system makes use of TCSpk from TPOINT<sup>™</sup>. A graphical user interface is provided for engineering

operation e.g. in stand-alone mode. In the normal operation mode, the UTCS is put under the control of the interferometer control system via a dedicated socket server.

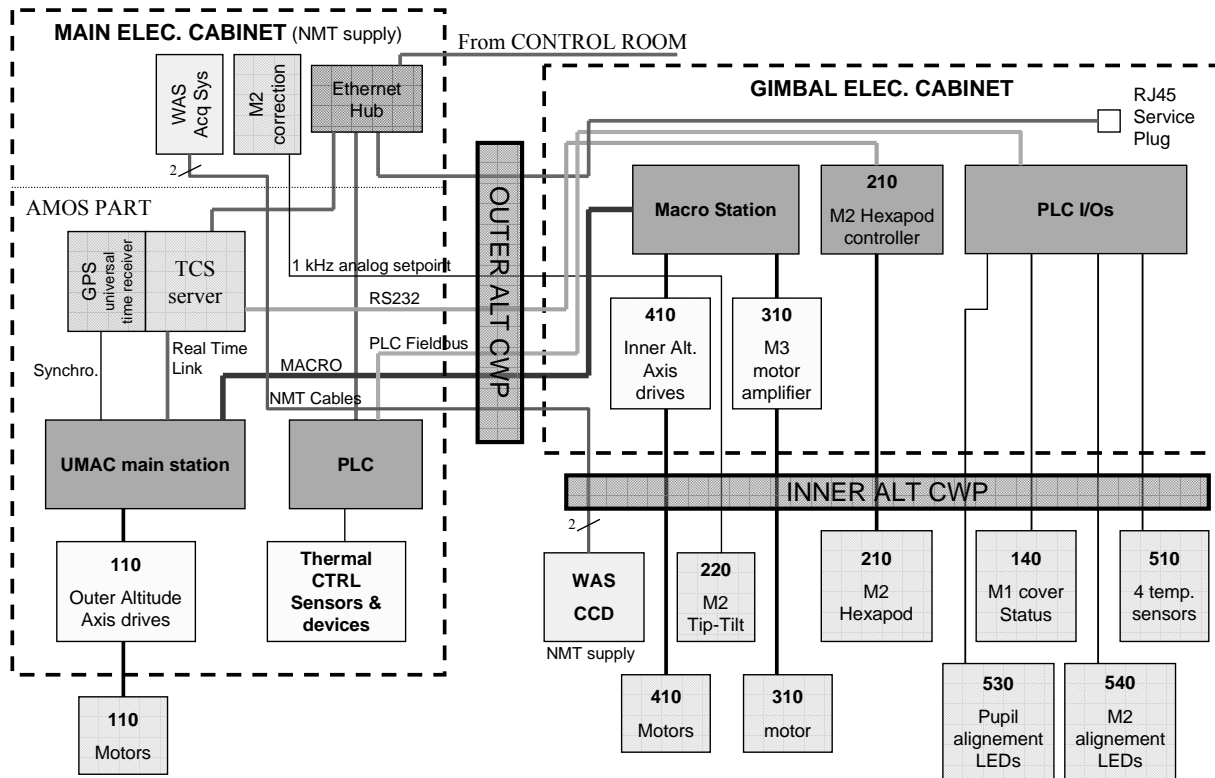


Fig. 12. Electronics: hardware deployment

#### 4. ENGINEERING APPROACH

One first crucial step in the design of an optical system is the optimization of the configuration with respect to the geometrical constraints. In the present case, the output beam and the tertiary mirror unit are fixed 1600 mm above the grade level. The question is to optimize the M1-M3 spacing on the criteria of the tube balancing while the output beam remains un-obstructed in any position of the field of regard. A CAD parametric model is employed to rapidly converge to an optimal configuration.

Then, a conceptual design is elaborated in order to start the analysis process. The loads applied to the telescope are determined by the environmental conditions (temperature, gravity, earthquake activity, wind speed) and the operational ranges. The optical quality, the pupil stability and the pointing error are affected by the static loads applied to the telescope. The tracking and the OPL stability performances result from the dynamic behavior of the system.

A Finite Element Model (FEM) is built and optimized on the criteria of the first frequencies (> 15 Hz, goal 20Hz) and the mirrors relative lateral displacements (goal < 50 μm). The first criterion is the simplest evaluation of the dynamic quality of the system; the second criterion provides information about the static deformation of the telescope for any pointing direction.

Since a specific error budget is allocated for the supporting of the primary, the design and the analysis of the M1 support can be done independently. The outcomes of the M1 analysis are however taken into account the budget consolidation.

For each system-level performance, the contributors are identified and an error budget is built. The sensitivity analysis determines quantitatively the weight of each contributor and shows possible schemes to improve the performance. For

this purpose, all the parameters affecting the optical performance are taken into account in the optical ZEMAX<sup>®</sup> models. Whenever it is necessary and possible, some compensation strategies are drawn up to meet the requirements.

The finite element static analysis under gravity and thermal load provides the relative displacement of the mirrors in the entire operational range. The image quality and the pupil stability are evaluated by adding these data to the other contributors such as the mirror surface quality, the axes run-out, etc.

The OPL stability under dynamic wind load is evaluated by a combination of FEA and frequency-domain post-processing. The method was successfully used for the auxiliary telescopes of the VLTI<sup>[3]</sup>.

The tracking performances are evaluated by the use of a SIMULINK<sup>®</sup> model. This model includes the controllers, the motors amplifiers, the telescope structure, the motors and the encoders of both axes.

An ultimate optimization is then necessary to meet all the requirements. In the following paragraph are briefly explained the optimization and compensation strategies put in place to meet the system level requirements.

The pupil stability is very sensitive to the rotational displacement of the tertiary. It was necessary to review the design of the spider and the attachment points to the structure in order to limit the displacement of M3.

The image quality requirements are very severe. The M1-M2 spacing shall be maintained within 2.2  $\mu\text{m}$  during observation. Of course, the structure deformation under gravity load and temperature changes is far higher than this requirement. A compensation law as a function of the temperature and the pointing direction will provide corrections to be applied to the position of the secondary mirror before starting an acquisition. The M2 hexapod allows proceeding to the same kind of correction to compensate the coma aberration.

The strategy to meet the tracking and OPL stability requirements is simple: maximizing the natural frequencies values of the telescope. Nevertheless, it is essential to identify the most significant modes for the OPL stability in regards with excitation and the pointing direction.

At the end of the optimization processes, the requirements for the sub-systems and the components are consolidated.

## 5. CONCLUSION

The elevation over elevation configuration necessitates a lot of care to attain a very good static and dynamic performance because of the unsymmetrical feature of the structure. However, the benefit for the optical throughput is significant and makes the design much simpler than an alt-azimuth mount.

AMOS uses the leading edge analysis techniques to produce reliable performance verifications. These techniques combine CATIA<sup>®</sup> for solid modeling, SAMCEF<sup>™</sup> for finite element analysis, ZEMAX<sup>®</sup> for the optical analyses and optimizations, MATLAB-SIMULINK<sup>®</sup> for the control system analysis and several in-house developed software for data post-processing and optimization. This approach is a must to produce a state of the art telescope within a short period of time.

The design phase of the MROI unit telescope is on the right way to be completed successfully within a few weeks.

## REFERENCES

- [1] Creech-Eakman, M. J., Bakker, E. J., Buscher, D. F., et al., "Magdalena Ridge Observatory interferometer: status update," Proc. SPIE 6268, -(2006)
- [2] Buscher, D. F., Bakker, E. J., Coleman, T. A., et al., "The Magdalena Ridge Observatory Interferometer: a high sensitivity imaging array," Proc. SPIE 6307, - (2006)
- [3] Delrez, C., Schumacher, J-M, Flebus, C., Gloesener, P., Koehler, B., "Optical path length calculation of the auxiliary telescope of the very large telescope project," Proc. 36<sup>th</sup> Liège International Astrophysical Colloquium, - (2002)
- [4] Mayer, C. J., et al., "The control system for the unit telescopes of the Magdalena Ridge Observatory interferometer," Proc. SPIE Vol. 7019, - (2008)